FEM Assisted Design and Simulation of Novel Electrothermal Actuators

S. Deladi, G. Krijnen and M. Elwenspoek

MESA+ Research Institute, University of Twente
P.O. Box 217, 7500 AE Enschede, The Netherlands
s.deladi@el.utwente.nl

ABSTRACT

In this work the authors present the design, simulation, and experimental results of novel electrothermal actuators, such as the trimorph actuator for out-of-plane motion, the coupled in-plane actuator for in-plane motion and an actuator providing combined in- and out-of-plane motion that have been developed for tribological studies. They can be easily embedded into complex MEMS devices due to the materials, which have been used for the fabrication. FEM simulations and experiments showed that the actuators are able to provide large forces to overcome adhesion and stiction.

Keywords: FEM simulation, trimproph actuator, out-of plane, in-plane, stiction, adhesion.

1 INTRODUCTION

The demand for powerful actuators, which can be embedded into MEMS devices draws attention to electrothermal actuators, although there can be drawbacks such as the heat generated during actuation. An appropriate design allows good temperature control over the entire structure and the main advantage is the low actuation voltage in comparison to electrostatic actuators.
Deflections and forces obtained by thermal expansion mismatch between materials are well known applications in the macro-world (thermocouples, bimetal beams, etc.), therefore in the past several investigations on their miniaturization have been reported [1,2,3].

Tribological experiments require in-plane and out-of plane motion to provide different testing conditions for adhesion, friction and wear studies. We report on actuators that have been developed to provide forces and deflections large enough for micro-tribological experiments. The out-of-plane actuator (trimorph) has to overcome adhesion between smooth surfaces and enable to quantify pull-off forces. The input parameters for the design of this actuator have been given by the computational results of an adhesional contact model between arbitrary rough surfaces reported on earlier [4].

To the best of our knowledge the material combination we used (fig. 2,3) is a novelty for actuation based on thermal expansion mismatch of resistively heated materials. The most important advantage is the embedding possibilities into MEMS devices conferred by the materials that have been used compared to other bimorph or multimorph structures [3,11]. With coupled electrothermal in-plane actuators (CETI) we provide the motion for friction and wear tests. It has been designed to increase the in-plane force (fig. 9,10) by adding individual contributions of electrothermal actuators [5,6]. By combining the trimorph and hot leg/cold leg actuators (CTHC), the tip of a new actuator moves on a 3D curve.

2 MATERIALS AND FABRICATION

All three actuators have been embedded into a fabrication process that allows their combination, subsequently in- and out-of-plane motions can be provided simultaneously for complex MEMS devices.

The material stack from which the actuators have been micromachined consists of a 1st 0.25 μm thick LPCVD Si-rich nitride (SiRN) layer deposited at 850 °C on a p-type Si wafer, a combination of LPCVD TEOS based (700 °C) and PECVD SiH_4 based (300 °C) silicon oxides for the 1st sacrificial layer of 2 μm thickness, a 1st 1.5 μm thick polycrystalline Si (polySi) layer deposited at 590 °C and locally doped with B, a 0.8 μm thick PECVD silicon oxide, a 2nd 0.25 μm SiRN, a 2nd sacrificial layer of LPCVD and PECVD silicon oxide combination (2 μm) and a 2nd locally B doped polySi layer of 2 μm thickness. The technological solutions for the fabrication as well as the advantage of using combined LPCVD and PECVD silicon oxide sacrificial layer have been reported on earlier [10].

The properties of the materials are of high importance for the performance simulation of the actuators with FEM (ANSYS). The available data about thermal properties of these materials are within wide range, however the data on mechanical properties are in relative good agreement and therefore these have been taken from the literature. The properties of the silicon oxide determined the choice of using it due to the lowest linear thermal expansion coefficient for known materials, low thermal conductivity compared to polySi, and the electrical insulating property.

For the design step of the actuators constant linear thermal expansion coefficients of the materials (α) have been considered (at room temperature), which simplified the computations. The results have been used as feedback for changing the geometrical characteristics of the actuators. Nevertheless, for the simulation of the fabricated actuators the temperature dependence of the linear thermal expansion coefficient $\alpha(T)$ of the materials has been used. Due to the good agreement in the literature on the thermal

properties of the silicon oxide, $\alpha(T)$ is used from [7]. Different $\alpha(T)$ have been found in the literature for Si and polySi [2,8,9], therefore we had to find the most appropriate one for our doped polySi. The vertical deflection of a doubly clamped beam has been measured at near melting temperature with a micrometer (resolution - 1 μm) mounted on an optical microscope and the measurements have been compared with analytical calculation of the deflection considering different $\alpha(T)$ from the literature. A match of 96% was found for $\alpha(T)$ from [8].

The role of the SiRN is to protect the silicon oxide during sacrificial etching, to electrically isolate other MEMS structures from the trimorph actuator during contact and to diminish heat conduction due to the lower thermal conductivity compared to polySi. However, as a side effect the range of out-of-plane deflection has been reduced and the structural normal force of the actuator has been increased. In the simulations linear variation of $\alpha(T)$ has been considered for SiRN, as fig. 1 shows. Other important properties [7,12] used in the simulation are presented in table 1.

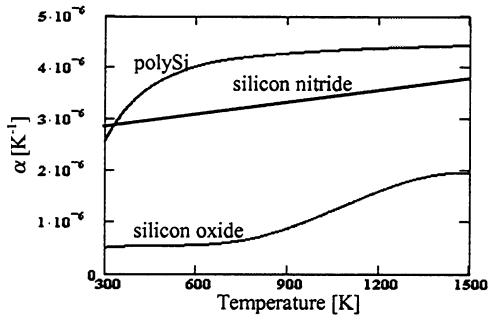

Figure 1: Temperature dependence of α.

Tabel 1: Material properties.

	polySi	SiRN	Si oxide
Young modulus [Pa]	$169 \cdot 10^9$	$270 \cdot 10^9$	$70 \cdot 10^9$
Poisson ratio	0.22	0.27	0.17
therm. conduct. [W/mK]	150	1.9	1.1

3 TRIMORPH ACTUATOR

The structure of the trimorph and CTHC actuators are micromachined from the doped areas of the 1st polySi layer, the PECVD silicon oxide and the 2nd SiRN layers. The actuator consists of two symmetric legs of polySi (length - 250 μm; width - 14 μm; gap between legs - 2 μm), upon which silicon oxide has been patterned (length – 244 μm; width - 8 μm), and finally the legs have been completely covered with SiRN (fig. 2 and 3). The out-of-plane motion is gained mostly from the thermal expansion mismatch of the doped polySi and the silicon oxide, but the SiRN has a damping effect.

Figure 2 shows the simulation of the actuator at operation near to failure. The temperature distribution (fig. 4) shows that the maximum temperature is obtained at the tip of the actuator where the symmetric legs are connected with a 4-μm wide polySi beam. The graph also shows the efficiency of the contact pads as heat sinks.

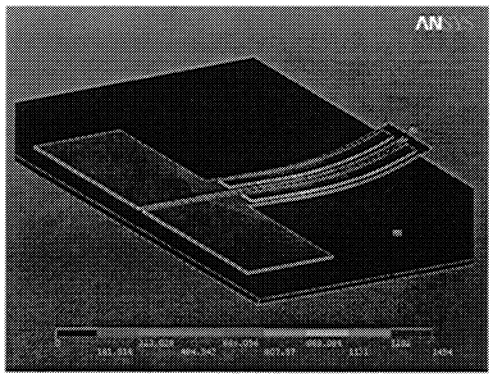

Figure 2: Simulation trimorph actuator – temperature distribution at 15V DC actuation.

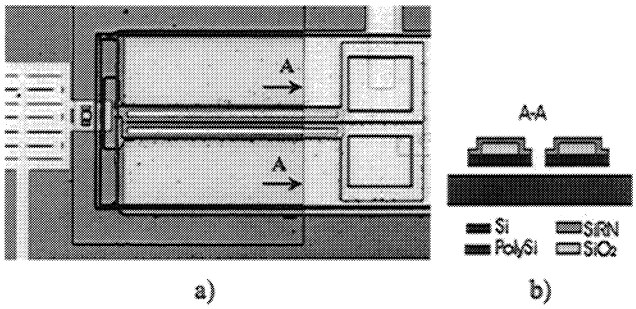

Figure 3: Trimorph actuator; a) fabricated; b) cross section.

The resistivity of the doped polySi has been found from matching the maximum operational temperature of the tested actuator to the simulated one at the same actuation voltage of 15 V DC. The limitation of the actuation seems to be caused by the softening of the silicon oxide and the increase of its α, because the failure of the actuator occurs when the softened silicon oxide breaks the polySi/SiRN interface (fig. 5). This temperature is estimated to be around 1400-1450 K, but it is certainly below the melting point of the polySi, because no harm to the polySi has been observed.

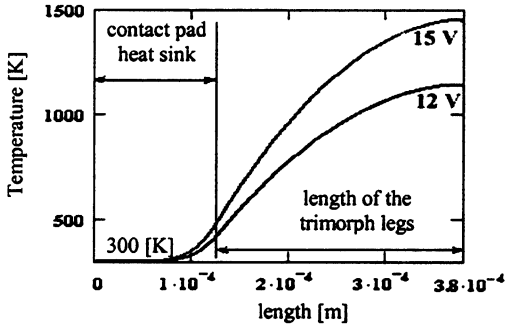

Figure 4: Temp. distribution along the actuator.

FEM simulations of the actuator have been performed for a range of actuation voltage, the results have been compared with the experimental ones (fig. 6.) and the voltage-displacement graph shows good agreement.

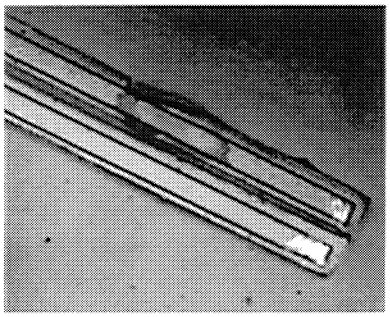

Figure 5: Failure of the trimorph actuator - at 15V DC.

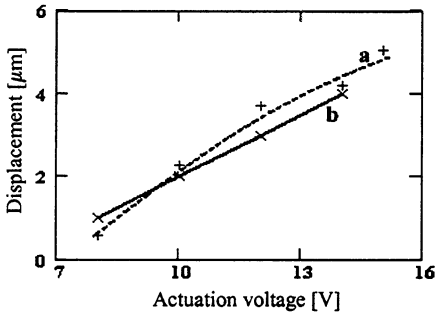

Figure 6: Voltage-displacement characteristic;
a - simulation; b - experimental results.

Other simulation results, such as the structural normal force at zero deflection (when actuation starts) and the maximum temperature at the tip of the actuator are given in fig. 7.
A comparison of the experimental results of the above described trimorph actuator and its 1.3 times scaled up version (in x and y directions) shows that larger displacement range can be achieved at the same actuation power for scaled up actuators (fig. 8).

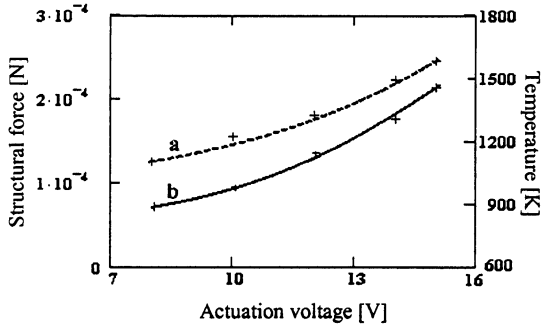

Figure 7: FEM simulated characteristics;
a – structural force; b – maximum temperature.

The influence of the SiRN layer can be observed from a comparison between the simulation of two geometrically identical actuators with and without SiRN capping. For actuation at 15 V DC at which the maximum temperature of both actuators is around 1500 K, the tip displacement of the trimorph actuator is 5.05 μm while that of the bimorph actuator is 26.9 μm, but for the last one the structural force decreases to one tenth of the first one at zero deflection.

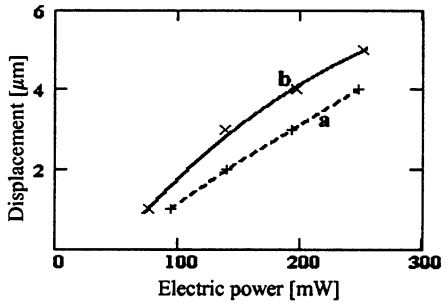

Figure 8: Experimental results; a – normal actuator;
b – 1.3 times scaled up (x and y directions).

4 CETI ACTUATOR

For the CETI actuator (fig. 10), the doped areas of the 1st polySi layer make the electrical contact between the left contact pad and the right electrodes of each individual actuator, than the electrical circuit between the right contact pad and the left electrodes is patterned together with the actuators and the connecting beam in the 2nd polySi layer. The 1st polySi layer is not doped underneath the actuator to avoid pull-in during operation and also the connecting beam consists of non doped polySi to avoid electrical connection between the individual actuators. The motion is generated due to the differential expansion of a hot (2 μm wide) and a cold (14 μm wide) leg. The tips of six actuators are connected to a beam (fig. 9), so that the force of the actuator is the sum of the individual contribution of the hot/cold leg actuators. The in-plane force of the CETI actuator is 81 μN if the length of the hot/cold legs is 250 μm and the thickness of the polySi is 2 μm.

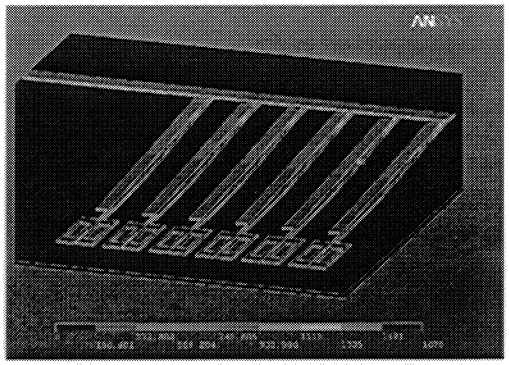

Figure 9: Simulation of CETI actuator. Temperature distribution at 23V DC actuation.

The voltage/displacement characteristic of the actuator, fig. 11, shows a comparison between simulated and

experimental results. The input electric power increases from 135.6 mW for a displacement of 2 μm to almost 450 mW for 8 μm, which was the maximum deflection before the melting temperature of the polySi has been reached. The increased rigidity of the structure diminishes the magnitude of the in-plane motion, taking the actuators separately the deflection is as much as 12.1 μm for the maximum actuation voltage.

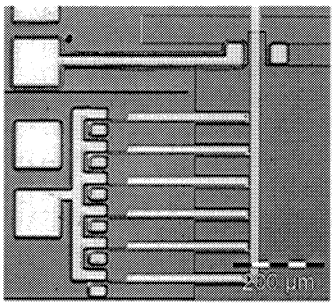

Figure 10: Fabricated CETI actuator.

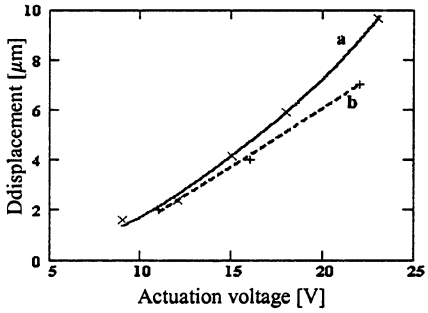

Figure 11: Voltage-displacement characteristic; a – simulation; b – experimental results.

4 CTHC ACTUATOR

The in-plane motion due to differential expansion of the legs and the out-of-plane motion due to thermal expansion mismatch of the materials are obtained simultaneously, the difference in magnitude depends on the geometrical characteristics of the actuator as well as the thickness of the layers. The CTHC actuator (fig. 12) is not very efficient if SiRN capping is used, the out-of-plane/in-plane deflection ratio decreases to 0.1 compared to 0.5 for the bimorph cold leg, at the same actuation voltage. This occurs due to the temperature distribution within the actuator, the maximum temperature is attained at the middle of the hot leg as it can be seen in fig. 12, therefore the bimorph or trimorph leg can not work with high efficiency. In this case the melting temperature of the polySi determines the failure of the actuator.

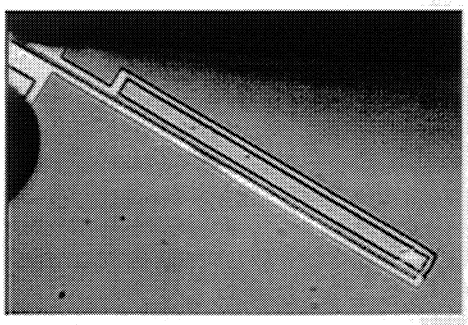

Figure 12: Actuation of CTHC actuator at 12 V DC.

CONCLUSIONS

The results of the preliminary FEM simulations have been used as input for the design of the novel actuators, then the performance of the actuators have been simulated taking into account the temperature dependence of the linear expansion coefficient of the materials.

The simulations are in relative good agreement with the experimental results, however for a better fit the temperature dependence of other properties such as the thermal conduction, resistivity and Young modulus of the materials has to be included in the model as well.

The trimorph actuator is able to provide the range of forces needed to pull-off smooth surfaces [1], therefore it is suitable for adhesion studies and moreover experiments showed that it is strong enough to release itself once it is kept to the substrate by stiction.

ACKNOWLEDGEMENTS

The authors would like to acknowledge the TST and MESA+ technical staff for useful discussions and the financial support of the Dutch Technology Foundation (STW).

REFERENCES

[1] J.M. Noworolski, Sensors and Actuators A55, 65-69, 1996.

[2] H. Tada, et.al., J. of Applied Physics, Vol.87, No. 9, 4189-4193, 2000.

[3] H. Sehr, et.al., J. Micromech. Microeng. Vol.11, 1306-1310, 2001.

[4] S. Deladi, et.al., Proc. ICCN'02, 326-329, 2002.

[5] E.S. Kolesar, et.al., Thin Solid Films 355-356, 295-302, 1999.

[6] M. Pai, et.al., Sensors and Actuators 83, 237-243, 2000.

[7] M. Bargmann, et.al., Mat. Res. Soc. Symp. Proc. Vol. 605, 235-240, 2000.

[8] Y. Okada, et.al., J. Appl. Phys. 56/2, 314-320, 1984.

[9] C.H. Pan, J. Micromechanics Microeng. 12, 548-555, 2002.

[10] S. Deladi, et.al., Proc. MME'02, 63-66, 2002.

[11] M. Ataka, et.al., J. of MEMS, Vol.2/4, 146-150, 1993.

[12] S.D. Senturia, Microsystem Design, Kluwet Academic Publisher, ISBN 0-7923-7246-8, 2000.